Research Paper

Synthesis and application of magnetized nanoparticles to remove lead from drinking water: Taguchi design of experiment

Muhammad Irfan Jalees

ABSTRACT

Contamination in drinking water from heavy metals like Pb^{2+} has severe effects on health. In this study, potato peel (PP) was used as the substrate and magnetic iron nanoparticles (MI) were deposited on PP using a co-precipitated method. Fourier transformation infrared spectroscopy (FTIR) and X-ray diffraction (XRD) analysis confirmed the deposition of MI on PP. The L16 (4^4) method of Taguchi design of experiment (DOE) was used for the optimization of adsorption condition, i.e., at 6 pH, 10 min of contact time, and a dose of 15 g/L can give more than 90% removal efficiency of Pb^{2+} using PP-MI. Contour maps, Taguchi response analysis, and analysis of variance (ANOVA) suggested that pH has a dominant contribution in the removal of Pb^{2+}. The adsorption process was favorable, spontaneous, and exothermic in nature and was followed by pseudo second order kinetics. A comparison of the sorption capacity of PP-MI for Pb^{2+} with literature values suggested that PP-MI has good potential for the removal of Pb^{2+}.

Key words | agro-nanoparticles, design of experiments (DOE), drinking water, Pb^{2+}, Taguchi method

Muhammad Irfan Jalees
Institute of Environmental Engineering and Research,
University of Engineering and Technology,
Lahore 54890,
Pakistan
E-mail: *irfan611@gmail.com*

This article has been made Open Access thanks to the generous support of a global network of libraries as part of the Knowledge Unlatched Select initiative.

INTRODUCTION

The cumulative, non-biodegraded, and persistent nature of heavy metals make them an environmental concern even when present in trace amounts (Gupta & Ali 2004). Exposure to heavy metal like Pb^{2+}, even in trace amounts, can cause adverse health effects (Gupta & Ali 2004). Many industries discharge industrial effluents containing Pb^{2+}, which can pose a risk to humans. Therefore, the treatment of Pb^{2+} prior to discharge is important, but the complex composition of effluents makes treatment difficult (Gupta & Ali 2004). Furthermore, the presence of dissolved organic compounds plays a key role in controlling the physiochemical properties of Pb^{2+} ions which further enhance the difficulty level for Pb^{2+} treatment (Gupta & Ali 2004). Out of many treatment methods, adsorption is considered as economic, efficient, and effective for the treatment of heavy metals (Günay *et al.* 2007; Feng *et al.* 2010; Dawodu *et al.* 2012). In the last decade, researchers have improved the quality and cost-effectiveness of adsorbent in the form of zeolites (Panuccio *et al.* 2009), clay minerals (Hizal & Apak 2006; Dawodu *et al.* 2012), and organic waste (Mackay *et al.* 1997). Although these adsorbent techniques are good, because of less surface area, expense, and generation of secondary waste, researchers are now using nano adsorbents (Chang & Chen 2005; Banerjee & Chen 2007; Badruddoza *et al.* 2011), nano alumina (Mahdavi *et al.* 2013), functionalized carbon nanotubes (Abbas *et al.* 2016), and hydroxyapatite nanoparticles (Mohammed *et al.* 2018). The high absorption abilities of nanoparticles are further

doi: 10.2166/washdev.2020.097

enhanced by the use of magnetic nanoparticles which increases the efficiency of solid–liquid separation problems (Plohl *et al.* 2019). These magnetic particles not only have a large surface area which increases the removal efficiency (%RE) but they are also easily prepared and can be separated from samples to reduce secondary solid waste generation (Plohl *et al.* 2019). Several attempts have been made to use various forms of nanoparticles, e.g., maghemite nanoparticles (Oukebdane *et al.* 2018), iron-humic acid, nanopolymers (Rao *et al.* 2019), etc. In this study, potato peel (PP) (agricultural waste) was used as substrate. Potato is abundantly used as potato chips. Based on the peeling method, 15–40% (% wt) of potato is wasted as potato peel. This potato peel is a major contributor of solid organic waste in food industries (Gebrechristos & Chen 2018). Using potato peel as a substrate will help in reducing solid waste. Magnetic iron (MI) particles were synthesized and coated on PP using the co-precipitated method. The PP-MI was also characterized using FTIR and XRD. The prepared PP-MI is then used as adsorbent material for optimization and isotherm studies for the removal of Pb^{2+} from drinking water.

MATERIAL AND METHODS

The chemicals used during experiments were $FeCl_3.6H_2O$, $FeSO_4.7H_2O$, ammonia solution, H_2SO_4, and $Pb(NO_3)_2$,were of analytical grade and purchased from Merck, Pakistan. The potato was purchased from the local market and its peel was used for experimentation. All glassware was Pyrex and washed with 2% HNO_3 and double rinsed with deionized water before being used in experimentation. The analysis of Pb^{2+} was performed on an Atomic Absorption Spectrometer (AAS) (Analyst 800, Perkin Elmer) (American Public Health Association 2005) in triplicate after performing the limit of detection (LOD) and quality checks (QC) test. Samples were also analyzed from the chemistry department, UET and Institute of Chemistry Punjab University (PU) to minimize errors. Characterization of PP-MI was performed using FTIR and XRD from the physics department, UET Lahore.

Preparation of the adsorbent

Potato peel (PP) was dried in sunlight for 8 hr daily for 6 days. The average temperature was 37–41 °C during the drying period. After drying, PP was transferred to an oven at 45 °C. The dried PP was then cut into small pieces, ground into powder form and stored in airtight jars to prevent damp. The mesh size of powdered PP was 60–200 micron. Powdered PP (1 g) was added into 200 mL of distilled water and heated at 80 °C. After that, 10 mL of NH_4OH was added to maintain a pH of 10. Ferrous sulfate hepta-hydrate (4.2 g) and ferric chloride hexa-hydrate (6.1 g) were mixed in 100 mL de-ionized water, separately. These salts were then slowly mixed with PP solution at 80 °C. After the complete addition of two iron salts, the combined solution was further heated for 30 min at 80 °C. The solution was cooled down and PP-MI nanoparticles were separated from the solution using a magnetic bar. PP-MI was dried and stored in airtight jars. Characterization of PP-MI was performed using FTIR (JASCO, FT/IR-4100 type A) and XRD (Shimadzu, XRD-7000). The composition of PP was determined in terms of carbohydrates (Dubois *et al.* 1956), proteins (Rice *et al.* 2017), fats (Soxhlet apparatus), ash, and metals (Rice *et al.* 2017).

Taguchi method for design of experiments (DOE)

Design of experiments (DOE) for the Taguchi method is used for the optimization of conditions. Four parameters, i.e., pH (2–8), dose of adsorbent (PP-MI) (5–20 g/L), contact time of adsorption (10–40 min) and initial concentration of Pb^{2+} (70–90 ppm) was selected. The method L16 (4^4) was selected for Taguchi DOE. It has four parameters and four levels. Table 1 contains the various inputs (16) for the

Table 1 | Composition of potato peel in terms of organic and inorganic content

Parameter	Mass %	Method
Moisture	83.29	ASTM D2216
Dry mass	16.71	ASTM D2216
Carbohydrates	10.66	ASTM D5896
Proteins (N_{tot})	1.38	ASTM D5712
Fats	0.43	ASTM D5555
Ash content	1.1	ASTM D5347
Calcium	0.75	*3,500 B Ca^{2+}
Magnesium	0.21	*3,500 B Mg^{2+}
Zinc	0.002	*3,500 B Zn^{2+}

*Standard methods for the examination of water and wastewater, 20th edition.

optimization of adsorption conditions. Known solutions of various Pb^{2+} concentrations (10–90 ppm) were prepared using the standard solutions provided by Perkin Elmer, US (Oukebdane *et al.* 2018). Analysis of iron which may be leached out during the adsorption process was also carried out using an atomic absorption spectrometer.

RESULTS AND DISCUSSION

Characterization of PP-MI

Chemical analysis of PP was performed to measure moisture content, carbohydrates, proteins, fats, ash, and heavy metals. The results of the composition are given in Table 1. FTIR analysis of PP and PP-MI indicated the binding of iron magnetic particles on PP. The infrared spectra of PP and PP-MI are given in Figure 1. Both PP and PP-MI showed almost the same FTIR spectra except the broad OH peak of PP at 3,434.76 cm^{-1} (OH stretch) and a new peak of PP-MI at 575.15 cm^{-1} (Fe–O). This suggests that the interaction of the hydroxyl groups and metal-oxide was generated during the PP-MI synthesis. The characteristic peaks of XRD (Figure 2) at 6.17°, 44.46°, and 51.46° further supported the deposition of MI on PP. These peaks were characteristic peaks of iron nanoparticles (Gupta & Ali 2012).

Optimization of parameters

Sixteen experimental sets were applied for the removal of Pb^{2+} from the drinking water. Table 2 shows the %RE for each set. An overall %RE of 38–97 was obtained using these experimental sets. Based on the finding, experimental set 9 (Table 2) gives maximum %RE, i.e., 97%. It appeared that pH was an important parameter for controlling the process of adsorption. The increase in %RE indicated the competition of metal ions with H^{+} bound to the adsorbent surface. Table 2 showed that at 6 pH, only 10 min was required for the removal of Pb^{2+} from the solution which indicated that adequate active sites of adsorbent were available for the adsorption. Adsorbent dose (PP-MI) of 15 g/L gave maximum %RE because by increasing the quantity of PP-MI, more active sites are available to adsorb a large quantity of Pb^{2+}. Although the initial concentration of Pb^{2+} was high (100 ppm), due to a large number of active sites of PP-MI, Pb^{2+} ions were easily removed. Based on the finding of DOE, contour maps (Figure 3) were plotted for %RE and predicted the best conditions for the removal of Pb^{2+}. The plot of %RE between pH and adsorbent dose (PP-MI) (Figure 3(a)) suggested that pH 6 and dose value of 15 g/L gave up to 90% RE for Pb^{2+} whereas the same %RE can be obtained after 10 min and with 15 g/L of dose as per plot between time and adsorbent dose

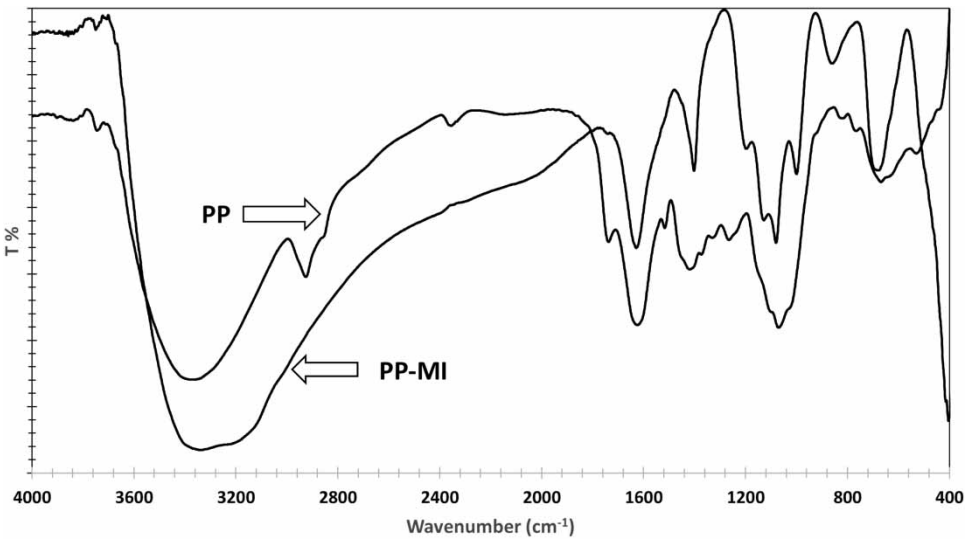

Figure 1 | FTIR spectra of PP and PP-MI showing the deposition of Fe on PP.

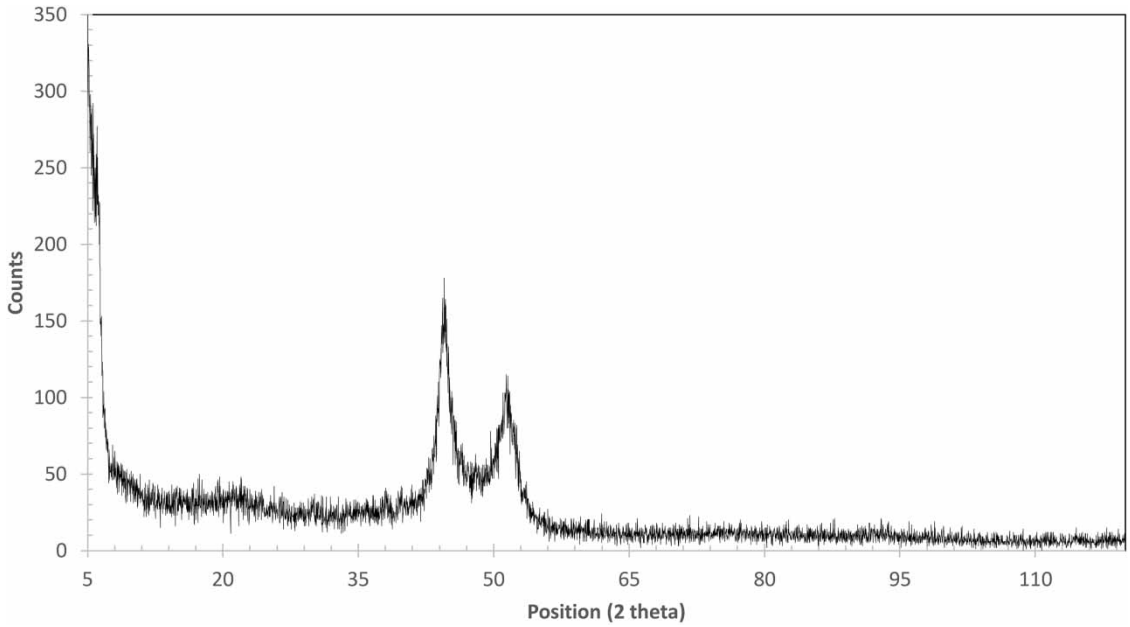

Figure 2 | XRD spectra of PP-MI. Potato peel (PP) did not show any XRD pattern due to the absence of any crystalline structure.

Table 2 | Removal efficiency of Pb^{2+} from drinking water using different experimental sets designed by the Taguchi method

Sr.	pH	Time (min)	Dose (g/L)	Conc. (ppm)	RE%
1.	2	10	5	70	42
2.	2	20	10	80	43
3.	2	30	15	90	38
4.	2	40	20	100	45
5.	4	10	10	90	60
6.	4	20	5	100	55
7.	4	30	20	70	58
8.	4	40	15	80	68
9.	6	10	15	100	97
10.	6	20	20	90	73
11.	6	30	05	80	54
12.	6	40	10	70	73
13.	8	10	20	80	71
14.	8	20	15	70	66
15.	8	30	10	100	63
16.	8	40	5	90	60

(Figure 3(b)). Furthermore, pH 6 and 15 g/L adsorbent dose along with 100 ppm concentration of Pb^{2+} also gave more than 90% removal efficiency of Pb^{2+} (Figure 3(d)).

Figure 4 was plotted using the Taguchi method result analysis and it confirmed that 6 pH (Figure 4(a)), 10 min time (Figure 4(b)), 15 g/L of adsorbent dose (Figure 4(c)), and 100 ppm Pb^{2+} (Figure 4(d)) concentration gave the maximum %RE. Further analysis of DOE results indicated that pH has a major effect on the %RE (Table 3) as it was ranked first in DOE result analysis. The significance of pH is also indicated by analysis of variance (ANOVA) (Table 4).

All %RE of all parameters were analyzed and only the pH has *significant* '*p*' value while all other parameters showed '*p*' values as *not significant*. This indicated that only the pH has a major effect on the removal of Pb^{2+} from drinking water using PP-MI particles.

Isotherm studies

Various isotherms, i.e., Langmuir isotherm, Freundlich isotherm, Temkin isotherm, Dubinin–Radushkevich (D-R) isotherm, and Flory–Huggins isotherm were used to study the mechanism of adsorption. These isotherms of adsorption are very important to discover the behavior of adsorbate on specific adsorbents. To find the maximum

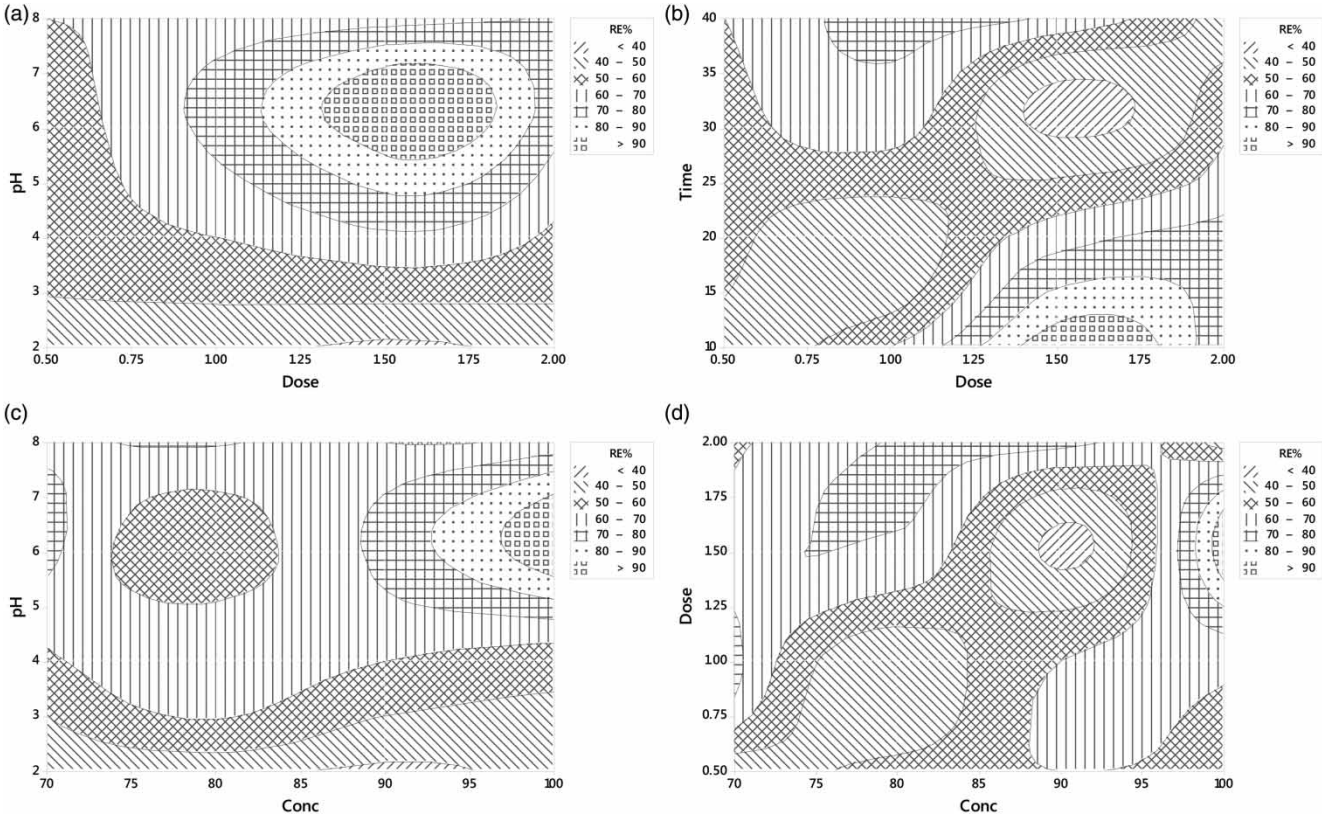

Figure 3 | Contour maps showing effects on removal efficiency using PP-MI: (a) pH vs dose of adsorbent; (b) time vs dose of adsorbent; (c) pH vs concentration of Pb^{2+}; (d) dose of adsorbent vs concentration of Pb^{2+}.

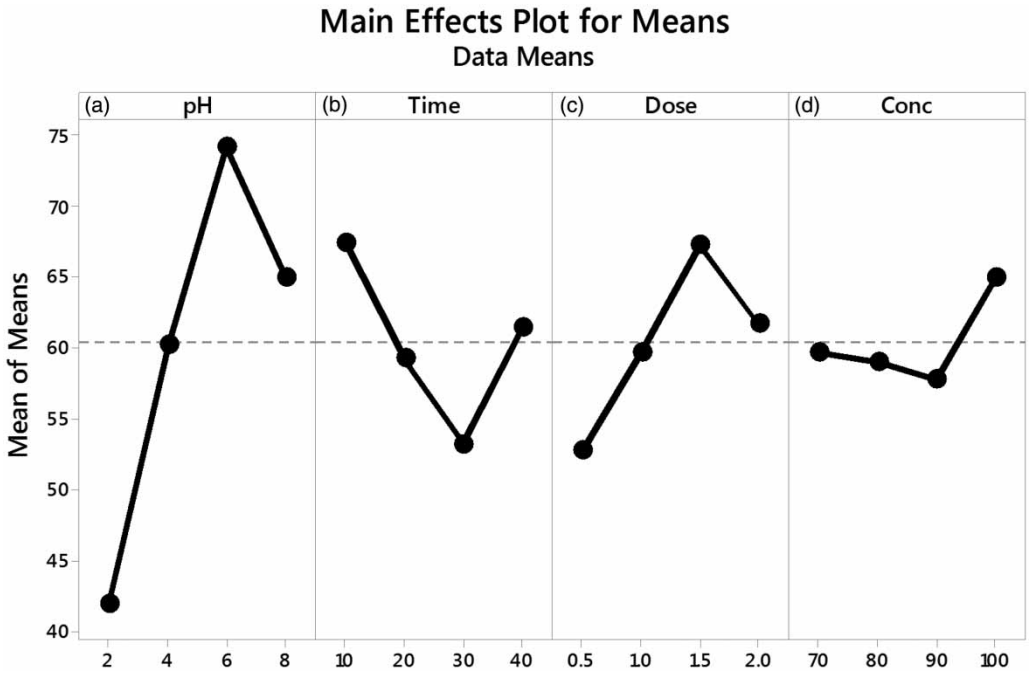

Figure 4 | Main effects plot for means of adsorption parameters for the removal of Pb^{2+} from drinking water: (a) pH; (b) time; (c) adsorbent dose; (d) concentration.

Table 3 | Analysis design of experiments (DOE) by Taguchi method to check maximum effect of parameters for %RE of Pb^{2+}

Level	pH	Time	Dose	Conc.
1	32.45	36.20	34.37	35.35
2	35.57	35.28	35.37	35.25
3	37.23	34.37	36.09	35.00
4	36.24	35.64	35.66	35.90
Delta	4.78	1.82	1.72	0.90
Rank	1	2	3	4

Table 4 | Analysis of variance (ANOVA) for design of experiments (DOE) by Taguchi method for significance of parameters for %RE of Pb^{2+}

Source	DF	Seq SS	Adj SS	Adj MS	F	P
pH	3	2,206.3	2,206.3	735.42	15.09	0.026
Time	3	416.2	416.2	138.75	2.85	0.207
Dose	3	430.7	430.7	143.58	2.95	0.199
Conc.	3	122.3	122.3	40.75	0.84	0.557

adsorption capacity of adsorbents, experiments are performed by varying metal ion concentrations and keeping all other parameters, i.e., pH (6), contact time (10 min), and adsorbent dose (15 g/L) at optimum. The isotherms show the relationship between the amount of Pb^{2+} taken up by per unit mass of adsorbent (q_e) and the equilibrium concentration of adsorbate in the bulk fluid phase (C_e). Table 5 contains the information for the construction of these adsorption models.

The Langmuir adsorption model was adopted for the homogenous monolayer adsorption process (Theivarasu & Mylsamy 2011). The model equation is given in Table 5. The linear plot of C_e vs C_e/q_e is given in Figure 5. The values (Table 6) of q_m and b were calculated using the slope and intercept of the plot (Figure 5(a)). The value of R_L was less than zero, which suggested the adsorption was favorable (Theivarasu & Mylsamy 2011).

The Freundlich isotherm model was adopted to calculate adsorption intensity on the adsorbent surface. The plot of $logC_e$ vs $logQ_e$ was used for this purpose (Figure 5(b)). The values of n and K_f were calculated from the slope and intercept of the graph, respectively. The value of n was smaller than zero, which suggested a favorable adsorption process.

The Dubinin–Radushkevich isotherm model was used for porosity and energy of adsorption measurements. The plot between ε^2 vs LnQ_e was used (Figure 5(c)). The values of K_{ad} and q_m were calculated using the slope and intercept of the graph, respectively (Table 6). The value of E (mean free energy of adsorption) was 0.32 kJ/mol.

The Temkin isotherm model was used to predict the uniform distribution of binding energy over the population of surface binding adsorption (Theivarasu & Mylsamy 2011). The plot of LnC_e vs Q_e was used (Figure 5(d)). The values

Table 5 | Mathematical models/equations for various isotherms used in the study

Sr.	Isotherm	Mathematical equation	Ref.
1.	Langmuir	$\frac{C_e}{q_e} = \frac{C_e}{q_m} + \frac{1}{q_m \times b}$ (1)	Jalees *et al.* (2019)
2.	Freundlich	$logq_e = logK_f + \frac{1}{n}\log C_e$ (2)	
3.	Temkin	$q_e = \beta\ln\alpha + \beta\ln C_e$ (3)	
4.	Dubinin–Radushkevich (D-R)	$lnq_e = ln(q_s) - (K_{ad}\varepsilon^2)$ (4)	
5.	Flory–Huggins	$log\frac{\theta}{Co} = \log K_{FH} + \text{n. log}(1-\theta)$ (5)	

Equation (1): [1] C_e: Equilibrium concentration of adsorbate (mg/L); q_e: amount of metal adsorbed per gram of adsorbate at equilibrium; q_m: maximum monolayer coverage capacity (mg/g); b: Langmuir isotherm constant.
Equation (2): K_f: Freundlich isotherm constant; n: adsorption intensity.
Equation (3): β: Temkin constant.
Equation (4): q_s: theoretical isotherm saturation capacity; K_{ad}: Dubnin–Radushkevich isotherm constant; ε: Dubnin–Radushkevich.
Equation (5): θ: degree of surface coverage; n: number of ions occupying adsorption sites; K_{FH}: Flory–Huggin isotherm constant.

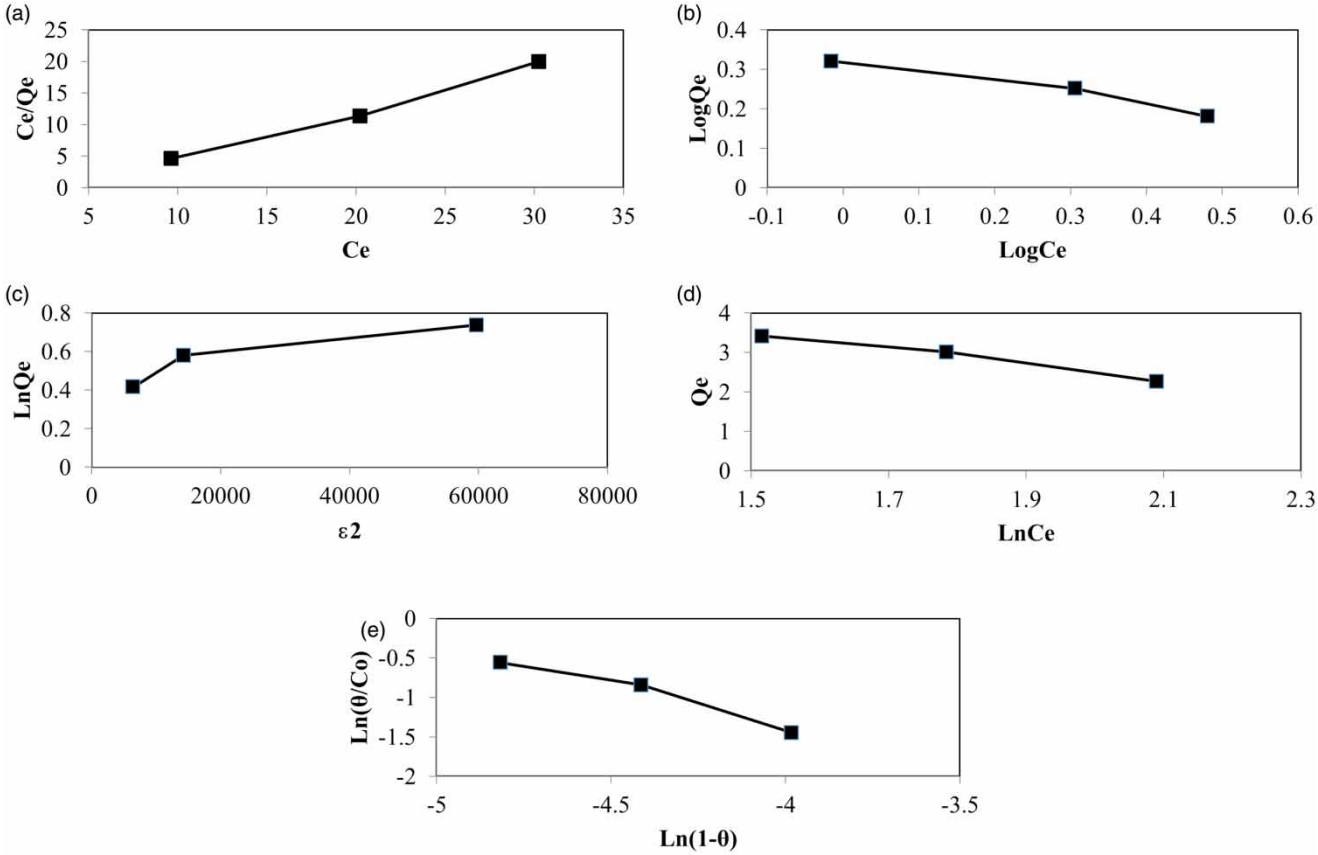

Figure 5 | Isotherms' response for the removal of Pb^{2+} using PP-IM: (a) Langmuir isotherm; (b) Freundlich isotherm; (c) Dubinin–Radushkevich isotherm; (d) Tempkin isotherm; (e) Florry Huggins isotherm. Calculated values for various isotherms are given in Table 6.

of α and β were calculated using the slope and intercept of the plot, respectively (Table 6).

The Flory–Huggins isotherm model was used for the degree of surface coverage of adsorbate on the adsorbent. The plot of $Ln(1-\theta)$ vs $Ln(\theta/C_o)$ was used (Figure 5(e)). The values of K_{FH} and n can be calculated by slope and intercept, respectively (Table 6). The value of ΔG indicated a spontaneous exothermic condition.

Kinetics

Kinetics of removal of Pb^{2+} was studied at optimized condition (mentioned in the previous section) at a concentration of 60 ppm of Pb^{2+}. The pseudo first order (Equation (6)) and pseudo second order (Equation (7)) kinetics were studied using the following equations (Jalees *et al.* 2019):

$$\frac{dq_t}{dt} = K_1(q_e - q_t) \tag{6}$$

$$\frac{dq_t}{dt} = K_2(q_e - q_t)^2 \tag{7}$$

The plot of t vs $log(Q_e - Q_t)$ and t vs T/Q_t was used for pseudo first (Figure 6(a)) and second order (Figure 6(b)), respectively. Various kinetic parameters measured from these plots are given in Table 7. The regression values suggested that the adsorption followed pseudo second order kinetics as R^2 value was very close to 1.

Table 6 | Various constants and parameters calculated for different isotherm used for the removal study of Pb^{2+} using PP-IM

Langmuir		Freundlich		Dubinin–Radushkevich	
Slope	0.74	Slope	−0.27	Slope	5.00×10^{-06}
Intercept	−2.93	Intercept	0.32	Intercept	0.44
Q_{max}	1.35	N	−3.67	K	5.00
R^2	0.99	K_f	2.09	Q_m	1.55
B	−0.25	R^2	0.97	E	0.32
R_L	−0.086	–	–	R^2	0.85
Temkin		**Flory–Huggins**			
Slope	−2.0	Slope	−1.07		
Intercept	6.49	Intercept	−5.64		
R^2	0.98	R^2	0.97		
A	0.74	N	13.78		
B	6.49	K_{fh}	35.42		
–	–	ΔG	−12.81		

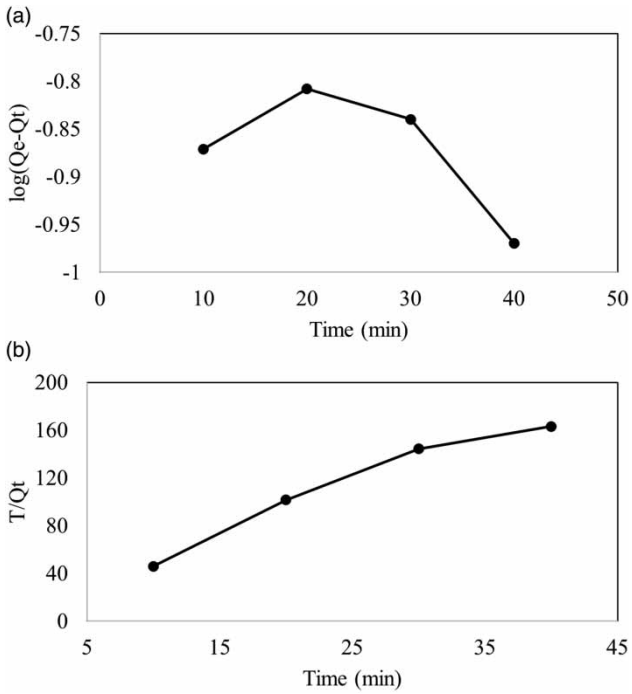

Figure 6 | Kinetics for the removal of Pb^{2+} using PP-MI: (a) pseudo first order; (b) pseudo second order.

Various researchers have used different nanoparticles for the removal of Pb^{2+} from drinking water (Table 8). A comparison of removal capacity by each methodology is given in Table 8. Simple nanoparticles to the composite nanoparticle, membrane/substrate supported nanoparticles, and bio-nanoparticles are available in the literature for the removal of Pb^{2+} in water. The removal capacity of PP-IM is better than the compared literature values which clearly indicates the good removal potential of PP-IM for Pb^{2+}.

Table 7 | Kinetics parameters for the removal of Pb^{2+} using PP-IM

Pseudo first order		Pseudo second order	
R^2	0.367	R^2	0.957
Q_e	0.454	Q_e	0.254
K1	0.003	K2	1.026
Q_e(exp)	0.353	Q_e(exp)	0.353

Table 8 | Comparison of removal capacity of PP-IM for Pb^{2+}

Adsorbent material	Pb^{2+} (mg/g)	Reference
PP-IM	97	Present study
Fe nanoparticles using C. lemon peel	59.4	Lung *et al.* (2018)
Fe iron particles	39	Moezzi *et al.* (2017)
L-Cyst-Fe_3O_4	18.8	Bagbi *et al.* (2017)
$MgFe_2O_4$–NH_2	10	Nonkumwong *et al.* (2016)
Polyaniline grafted chitosan	16.07	Karthik & Meenakshi (2015)
Sulfur-modified magnetic nanoparticle	14.03	Jafarinejada *et al.* (2017)
Nanostructured graphite oxide	82.59	Sheet *et al.* (2014)
Magnesium oxide nanoparticles	21.78	Dargahi *et al.* (2016)
Phyto-inspired iron oxide nanoparticles	93	Das & Rebecca (2018)

CONCLUSION

The use of agro-nanoparticles for the removal of Pb^{2+} from drinking water shows good results. Characteristic peaks of FTIR and XRD confirmed the deposition of MI on PP. The Taguchi design of experiment (16 experiments) was performed, which indicated that at pH 6, the contact time of 10 min and an adsorbent dose of 15 g/L can give more than 90% removal efficiency of Pb^{2+} using PP-MI. Contour

maps, Taguchi response analysis, and ANOVA showed the dominant contribution of pH in the removal of Pb^{2+} from drinking water. Isotherm studies indicated that the adsorption process was favorable and consists of heterogeneous binding sites of multilayers adsorbent with 0.32 KJ/mol free energy as a spontaneous exothermic process. Kinetics studies showed that the adsorption process was followed by pseudo second order kinetics. A comparison of the sorption capacity of PP-MI for Pb^{2+} with literature values suggested that PP-MI has good potential for the removal of Pb^{2+} from drinking water. The overall results indicated that the use of potato peel (considered as waste) as a substrate for nanoparticles will be helpful in the treatment of heavy metals in water.

REFERENCES

Abbas, A., Al-Amer, A. M., Laoui, T., Al-Marri, M. J., Nasser, M. S., Khraisheh, M. & Atieh, M. A. 2016 Heavy metal removal from aqueous solution by advanced carbon nanotubes: critical review of adsorption applications. *Separation and Purification Technology* **157**, 141–161.

American Public Health Association 2005 *3500 B Pb Standard Methods for the Examination of Water and Wastewater*. American Public Health Association (APHA), Washington, DC, USA.

Badruddoza, A., Tay, A., Tan, P., Hidajat, K. & Uddin, M. 2011 Carboxymethyl-β-cyclodextrin conjugated magnetic nanoparticles as nano-adsorbents for removal of copper ions: synthesis and adsorption studies. *Journal of Hazardous Materials* **185** (2), 1177–1186.

Bagbi, Y., Sarswat, A., Mohan, D., Pandey, A. & Solanki, P. R. 2017 Lead and chromium adsorption from water using L-cysteine functionalized magnetite (Fe3O4) nanoparticles. *Scientific Reports* **7** (1), 7672. doi:10.1038/s41598-017-03380-x.

Banerjee, S. S. & Chen, D.-H. 2007 Fast removal of copper ions by gum arabic modified magnetic nano-adsorbent. *Journal of Hazardous Materials* **147** (3), 792–799.

Chang, Y.-C. & Chen, D.-H. 2005 Preparation and adsorption properties of monodisperse chitosan-bound Fe_3O_4 magnetic nanoparticles for removal of Cu (II) ions. *Journal of Colloid and Interface Science* **283** (2), 446–451.

Dargahi, A., Golestanifar, H., Darvishi, P., Karami, A., Hasan, S. H., Poormohammadi, A. & Behzadnia, A. 2016 An investigation and comparison of removing heavy metals (lead and chromium) from aqueous solutions using magnesium oxide nanoparticles. *Polish Journal of Environmental Studies* **25** (2), 557–562.

Das, M. P. & Rebecca, L. J. 2018 Removal of lead (II) by phyto-inspired iron oxide nanoparticles. *Nature Environment and Pollution Technology* **17** (2), 569–574.

Dawodu, F., Akpomie, G. & Ogbu, I. 2012 Isotherm modeling on the equilibrium sorption of cadmium (II) from solution by agbani clay. *International Journal of Multidisciplinary Science and Engineering* **3** (9), 9–14.

Dubois, M., Gilles, K. A., Hamilton, J. K., Rebers, P. T. & Smith, F. 1956 Colorimetric method for determination of sugars and related substances. *Analytical Chemistry* **28** (3), 350–356.

Feng, Y., Gong, J.-L., Zeng, G.-M., Niu, Q.-Y., Zhang, H.-Y., Niu, C.-G., Deng, J.-H. & Yan, M. 2010 Adsorption of Cd (II) and Zn (II) from aqueous solutions using magnetic hydroxyapatite nanoparticles as adsorbents. *Chemical Engineering Journal* **162** (2), 487–494.

Gebrechristos, H. Y. & Chen, W. 2018 Utilization of potato peel as eco-friendly products: a review. *Food Science & Nutrition* **6** (6), 1352–1356.

Günay, A., Arslankaya, E. & Tosun, I. 2007 Lead removal from aqueous solution by natural and pretreated clinoptilolite: adsorption equilibrium and kinetics. *Journal of Hazardous Materials* **146** (1), 362–371.

Gupta, V. K. & Ali, I. 2004 Removal of lead and chromium from wastewater using bagasse fly ash – a sugar industry waste. *Journal of Colloid and Interface Science* **271** (2), 321–328.

Gupta, V. K. & Ali, I. 2012 *Environmental Water: Advances in Treatment, Remediation and Recycling*. Elsevier, Amsterdam, The Netherlands.

Hizal, J. & Apak, R. 2006 Modeling of cadmium (II) adsorption on kaolinite-based clays in the absence and presence of humic acid. *Applied Clay Science* **32** (3), 232–244.

Jafarinejada, S., Farajib, M., Jafaria, P. & Mokhtari-Aliabadc, J. 2017 Removal of lead ions from aqueous solutions using novel-modified magnetic nanoparticles: optimization, isotherm, and kinetics studies. *Desalination and Water Treatment* **92**, 267–274.

Jalees, M. I., Farooq, M. U., Basheer, S. & Asghar, S. 2019 Removal of heavy metals from drinking water using Chikni Mitti (kaolinite): isotherm and kinetics. *Arabian Journal for Science and Engineering*. https://doi.org/10.1007/s13369-019-03722-z

Karthik, R. & Meenakshi, S. 2015 Removal of Pb (II) and Cd (II) ions from aqueous solution using polyaniline grafted chitosan. *Chemical Engineering Journal* **263**, 168–177.

Lung, I., Stan, M., Opris, O., Soran, M.-L., Senila, M. & Stefan, M. 2018 Removal of lead (II), cadmium (II), and arsenic (III) from aqueous solution using magnetite nanoparticles prepared by green synthesis with Box–Behnken design. *Analytical Letters* **51** (16), 2519–2531.

Mackay, D., Shiu, W. Y. & Ma, K.-C. 1997 *Illustrated Handbook of Physical-Chemical Properties of Environmental Fate for Organic Chemicals*, Vol. 5. CRC Press, Boca Raton, FL, USA.

Mahdavi, S., Jalali, M. & Afkhami, A. 2013 Heavy metals removal from aqueous solutions using TiO_2, MgO, and Al_2O_3 nanoparticles. *Chemical Engineering Communications* **200** (3), 448–470.

Moezzi, A., Soltanali, S., Torabian, A. & Hassani, A. 2017 Removal of lead from aquatic solution using synthesized iron nanoparticles. *International Journal of Nanoscience and Nanotechnology* **13** (1), 83–90.

Mohammed, E., Bouazza, T. & Khalil, E.-H. 2018 Structural and vibrational study of hydroxyapatite bio-ceramic pigments with chromophore ions (Co^{2+}, Ni^{2+}, Cu^{2+}, Mn^{2+}). In: *Advanced Intelligent Systems for Sustainable Development, AI2SD 2018* (M. Ezziyyani eds). Advances in Intelligent Systems and Computing, Springer, Cham, Switzerland, pp. 62–70.

Nonkumwong, J., Ananta, S. & Srisombat, L. 2016 Effective removal of lead (II) from wastewater by amine-functionalized magnesium ferrite nanoparticles. *RSC Advances* **6** (53), 47382–47393.

Oukebdane, K., Belyouci, O. & Didi, M. A. 2018 Liquid-solid adsorption of Cd (II) by maghemite. *Current Nanomaterials* **3** (2), 95–102.

Panuccio, M. R., Sorgonà, A., Rizzo, M. & Cacco, G. 2009 Cadmium adsorption on vermiculite, zeolite and pumice: batch experimental studies. *Journal of Environmental Management* **90** (1), 364–374.

Plohl, O., Finšgar, M., Gyergyek, S., Ajdnik, U., Ban, I. & Fras Zemljič, L. 2019 Efficient copper removal from an aqueous environment using a novel and hybrid nanoadsorbent based on derived-polyethyleneimine linked to silica magnetic nanocomposites. *Nanomaterials* **9** (2), 209.

Rao, B. S., Kalahasti, S., Rao, E. V., Prasad, K. R. & Sandhya, J. 2019 Polymer nano composites for water pollution applications. *Journal of Water Pollution & Purification Research* **5** (3), 7–9.

Rice, E., Baird, R. & Eaton, A. 2017 *Standard Methods for the Examination of Water and Wastewater*. American Water Works Association, Washington, DC, USA.

Sheet, I., Kabbani, A. & Holail, H. 2014 Removal of heavy metals using nanostructured graphite oxide, silica nanoparticles and silica/graphite oxide composite. *Energy Procedia* **50**, 130–138.

Theivarasu, C. & Mylsamy, S. 2011 Removal of malachite green from aqueous solution by activated carbon developed from cocoa (Theobroma Cacao) shell-A kinetic and equilibrium studies. *Journal of Chemistry* **8** (S1), S363–S371.

First received 20 August 2019; accepted in revised form 29 November 2019. Available online 13 January 2020